Defect modes due to substitutional anion-pair and cation-pair impurities in ionic crystals

R. K. Gupta* and P. Mathur
Department of Physics, University of Jodhpur, Jodhpur-342001, India
(Received 23 August 1979)

Defect modes due to substitutional anion- as well as cation-pair impurities aligned in the [110] direction in various alkali-halide crystals have been computed using the Green's-function technique and compared with experimental results. The following systems were studied: $KCl:H^-–H^-$, $KCl:D^-–D^-$, $KBr:H^-–H^-$, $KBr:D^-–D^-$, $RbCl:H^-–H^-$, $NaCl:H^-–H^-$, $KI:H^-–H^-$, $KI:Cl^-–Cl^-$, $KI:Br^-–Br^-$, $KI:Na^+–Na^+$, $KI:Rb^+–Rb^+$, $NaCl:F^-–F^-$, $NaCl:Ag^+–Ag^+$, and $KCl:Na^+–Na^+$. We have considered the vibrations of 12 particles, viz., the two-defect ions and their ten nearest neighbors; i.e., a 36×36-dimensional defect space has been used. Mass changes as well as the changes in the short-range interactions due to the introduction of defects have been taken into account. The system has D_{2h} site symmetry around the defect ions which has been used to block-diagonalize the relevant 36×36 matrix by employing group theory. Six irreducible representations thus obtained were used to compute the defect modes, three of which are infrared active while the remaining three are Raman active. Numerical values of the required Green's functions calculated on the basis of the neutron-fitted shell-model parameters were used. The computed modes are found to be in good agreement with the experimental values.

INTRODUCTION

When isolated point defects are introduced in an otherwise perfect crystal, it exhibits new vibrational modes called defect modes. In these modes the mode frequency lies outside the allowed bands of frequencies for the phonon propagation in the host crystal and hence the vibrations remain localized near the defect ions. Such modes are accordingly termed as the localized modes. Besides these, so-called resonance our qualilocalized modes can also occur, whose frequencies lie in the bands of allowed frequencies and which are characterized by a large amplitude of vibration of the defect atoms or of those atoms with which they interact directly. The experimental and the theoretical study of these modes has acquired much importance recently, owing to the fact that the introduction of an impurity as a "probe" in a lattice provides a direct technique for investigating the lattice forces.[1-4]

A wide variety of experimental techniques, such as specific-heat and thermal-conductivity measurements, infrared absorption, Raman spectroscopy, Mössbauer effect, etc., can be used to study these modes experimentally. Several experiments have recently been carried out on the localized and resonant modes due to pair impurities in ionic crystals. De Souza *et al.*[5-7] used the infrared-absorption method to measure the local mode frequencies in KCl and KBr containing $H^-–H^-$, $H^-–D^-$, and $D^-–D^-$ pair impurities along the [110] direction and also localized modes due to $H^-–H^-$ pairs in the [110] direction in NaCl, RbCl, and KI. From polarized-light measurements they have given unambiguous assignments to the observed peaks. Becker and Martin[8] observed resonant modes due to $F^-–F^-$ pairs in NaCl. Their experiments on infrared absorption revealed six peaks apart from the main resonant peak due to a single F^- ion impurity which they attributed to the presence of $F^-–F^-$ pairs in two configurations, viz., the [110] and [200] configurations. Resonant modes due to Na^+ ion pairs aligned in the [110] direction in KCl have been observed by Templeton *et al.*[9] while gap modes (localized modes whose frequencies lie in the gap between the acoustic and optical bands) due to Cl^-, Br^-, and Na^+ ion pairs in KI have been observed by Ward and Clayman[10] using the impurity-induced infrared-absorption method. Resonant modes due to Ag^+ ion pairs in NaCl have been observed by Moller *et al.*[11] using Raman spectroscopy.

To account for the observed modes due to $H^-–H^-$, $D^-–D^-$, and $H^-–D^-$ pairs, theoretically, de Souza *et al.* employed a coupled-harmonic-oscillator model. Ward and Clayman[12] have applied the molecular-model method to compute the gap modes due to Rb^+ ion pairs in KI. Haridasan *et al.*[13,14] applied a Green's-function technique to explain theoretically the observed defect modes of the systems $KCl:H^-–H^-$, $KCl:D^-–D^-$, and $NaCl:F^-–F^-$, but they considered the vibrations of only four particles, namely, the two defect ions and their two nearest neighbors only; i.e., they used only a 12×12-dimensional defect space, whereas a more realistic model would have been to consider the vibrations of the defect ions together with all their nearest neighbors. Earlier, we had reported[15] the results of our calcu-

lations of the defect modes due to H^-–H^- and D^-–D^- pairs in RbCl using a Green's-function technique and considering the vibrations of the defect atoms only, i.e., using only a 6×6-dimensional defect space.

In this paper we present our calculations of the defect modes, using a Green's-function technique, for the systems KCl : H^-–H^-, KCl : D^-–D^-, KBr : H^-–H^-, KBr : D^-–D^-, NaCl : H^-–H^-, RbCl : H^-–H^-, KI : H^-–H^-, KI : Cl^-–Cl^-, KI + Na^+–Na^+, KCl : Na^+–Na^+, NaCl : F^-–F^-, NaCl : Ag^+–Ag^+, KI : Br^-–Br^-, and KI : Rb^+–Rb^+, taking the defect ion pairs to be in the [110] direction. We consider the vibrations of 12 particles, viz., the two defect ions and their ten nearest neighbors, i.e., a 36×36-dimensional defect space is used. The system has D_{2h} site symmetry around the defect ions which can be exploited to block-diagonalize the relevant 36×36 matrix. Six irreducible representations are thus obtained in terms of the Green's functions of the perfect crystal and the elements of the perturbation matrix consisting of the mass changes and changes in the short-range interactions at the defect sites. These irreducible representations are used to compute the defect modes, three out of which are infrared active while the remaining three are Raman active. The calculated modes agree very well with the experimental values.

METHOD OF CALCULATION: THE GREEN'S-FUNCTION APPROACH

It is appropriate to begin with a brief resume of the dynamics of crystals containing point defects. It is well known[16] that in the harmonic approximation, the time-independent equation of motion for a perfect crystal containing N unit cells each of which has r atoms, can be written as

$$\underline{L}\,\underline{U}=\underline{0}\,,$$

where L denotes a $3rN\times 3rN$ matrix whose elements are given by

$$L_{\alpha\beta}(lk,l'k';\omega^2)=M_k\omega^2\delta_{ll'}\,\delta_{kk'}\,\delta_{\alpha\beta}-\phi^0_{\alpha\beta}(lk,l'k')$$

and $\underline{U}$ is a column vector with $3rN$ elements $U_\alpha(lk)$. Here $U_\alpha(lk)$ denotes the αth Cartesian component of the displacement from the equilibrium position for the kth atom in the lth unit cell, and the other symbols have their usual meanings. With the presence of the point defects, the corresponding equation for the perturbed crystal can be written as

$$(\underline{L}-\underline{\delta L})\underline{U}=\underline{0}\,. \tag{1}$$

The elements of the perturbation matrix $\underline{\delta L}$ are given by

$$\delta L_{\alpha\beta}(lk,l'k',\omega^2)=(M_k-M_{lk})\omega^2\delta_{ll'}\,\delta_{kk'}\,\delta_{\alpha\beta}-[\phi^0_{\alpha\beta}(lk,l'k')-\phi_{\alpha\beta}(lk,l'k')]\,.$$

Equation (1) can be written as $\underline{L}^{-1}\underline{\delta L}\,\underline{U}=\underline{U}$ or as

$$\underline{G}\,\underline{\delta L}\,\underline{U}=\underline{U}\,, \tag{2}$$

where $\underline{G}\equiv\underline{L}^{-1}$ is called the Green's-function matrix or the host crystal. An explicit expression for the elements of the matrix $\underline{G}$ is given by

$$G_{\alpha\beta}(lk,l'k',\omega^2)=\frac{1}{N(M_kM_{k'})^{1/2}}\times\sum_{\vec{K}j}\frac{e_\alpha(k\,|\,\vec{K}j)\cdot e^*_\beta(k'\,|\,\vec{K}j)}{\omega^2-\omega_j^2(\vec{K})}\times\exp\{i\vec{K}\cdot[\vec{X}(lk)-\vec{X}(l'k')]\}\,.$$

Here N is the number of unit cells in the crystal, $\vec{X}(lk)$ is the equilibrium position vector of the kth atom in the lth unit cell, M_k is the mass of the kth kind of ion, $\omega_j(\vec{K})$ is the normal-mode frequency of the crystal, described by the wave vector $\vec{K}$, and branch index j and $e_\alpha(k\,|\,\vec{K}_j)$ is the α-Cartesian component of the associated unit polarization vector.

The matrix $\underline{\delta L}$ can have at the most $3n\times 3n$ nonzero elements where n is the number of lattice sites directly touched by the presence of the defect ions including the defect ions themselves. For the present case $n=2+10=12$. Here 2 is the number of defect ions and 10 is the number of their nearest neighbors. We can now partition the $\underline{\delta L}$, $\underline{G}$, and $\underline{U}$ in terms of the $3n\times 3n$ space (called the defect space) and the rest of the space as follows:

$$\underline{\delta L}=\begin{pmatrix}\underline{J} & \underline{0}\\ \underline{0} & \underline{0}\end{pmatrix},\quad \underline{G}=\begin{pmatrix}\underline{g} & \underline{g}_{12}\\ \underline{g}_{21} & \underline{g}_{22}\end{pmatrix},\quad \underline{U}=\begin{pmatrix}\underline{U}_1\\ \underline{U}_2\end{pmatrix}.$$

Here $\underline{J}$, $\underline{g}$, and $\underline{U}_1$ are in the $3n\times 3n$ space. The set of $3rN$ equations (2) now separate into two sets of equations, viz.,

$$\underline{U}_1=\underline{g}\underline{J}\underline{U}_1\,, \tag{3}$$

$$\underline{U}_2=\underline{g}_{21}\underline{J}\underline{U}_1\,. \tag{4}$$

The set of equations (3) comprises a set of $3n$ homogeneous equations for the $3n$ displacements of n particles constituting the defect space. A nontrivial solution for these $3n$ displacements exists only if the determinant of their coefficients vanishes; i.e.,

$$|\underline{I}-\underline{g}\underline{J}|=0\,, \tag{5}$$

where $\underline{I}$ is the $3n\times 3n$ unit matrix.

The determinantal equation (5) is the basic equation for the computation of defect modes due to point defects in otherwise perfect crystals. Further simplification is achieved by exploiting the symmetry involved in the problem. Figure 1 de-.

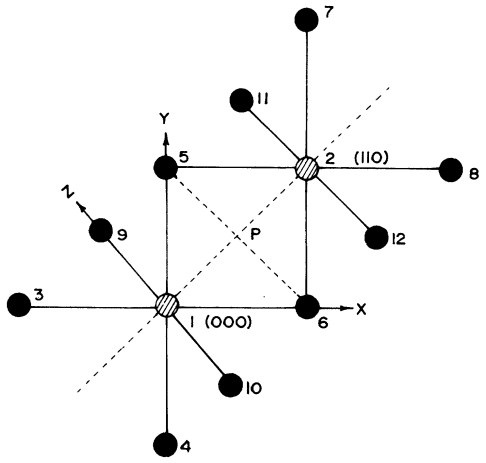

FIG. 1. 12-particle system comprising the defect space.

picts the defect ions together with their nearest neighbors in the equilibrium configuration. Particles 1(0,0,0) and 2(1,1,0) are the defect ions while the remaining 10 particles are their nearest neighbors in the host crystal. The system has D_{2h} site symmetry around the point P. The character table of the D_{2h} group can be used to construct the normal coordinates for the system from which one can construct the unitary matrix $\underline{U}$, which would, by a unitary transformation, block-diagonalize the 36×36 $(\underline{I}-\underline{GJ})$ matrix into eight irreducible representations as follows:

$$\Gamma_{36}=6A_g+5B_{1g}+3B_{2g}+4B_{3g}+2A_U+5B_{1U}+6B_{2U}+5B_{3U}.$$

The determinantal equation (5) separates into eight determinantal equations:

$$|A_g|=0,\quad |B_{1g}|=0,\quad |B_{2g}|=0,\quad |B_{3g}|=0,$$
$$|A_U|=0,\quad |B_{1U}|=0,\quad |B_{2U}|=0,\quad |B_{3U}|=0.$$

In the present case, the determinants $|B_{2g}|$ and $|A_U|$ are seen to be identically equal to unity, and hence the equations $|B_{2g}|=0$, $|A_U|=0$ give no modes.

The defect modes are thus analyzed in terms of the three Raman-active modes (A_g, B_{1g}, and B_{3g}) and the three infrared-active modes (B_{1U}, B_{2U}, and B_{3U}).

The elements of the six determinants are in terms of the elements of the $\underline{g}$ and $\underline{J}$ matrices. The elements of the $\underline{g}$ matrix for the anion-pair impurity can be written in terms of the following 26 independent Green's functions:

$$g_1=G_{xx}(000,-;000,-;\omega^2),$$
$$g_2=G_{xx}(000,+;000,+;\omega^2),$$
$$g_3=G_{xx}(000,-;100,+;\omega^2),$$
$$g_4=G_{yy}(000,-;100,+;\omega^2),$$
$$g_5=G_{xx}(000,-;110,-;\omega^2),$$
$$g_6=G_{xy}(000,-;110,-;\omega^2),$$
$$g_7=G_{zz}(000,-;110,-;\omega^2),$$
$$g_8=G_{xx}(000,+;110,+;\omega^2),$$
$$g_9=G_{xy}(000,+;110,+;\omega^2),$$
$$g_{10}=G_{zz}(000,+;110,+;\omega^2),$$
$$g_{11}=G_{xx}(000,-;111,+;\omega^2),$$
$$g_{12}=G_{xy}(000,-;111,+;\omega^2),$$
$$g_{13}=G_{xx}(000,+;200,+;\omega^2),$$
$$g_{14}=G_{yy}(000,+;200,+;\omega^2),$$
$$g_{15}=G_{xx}(000,-;210,+;\omega^2),$$
$$g_{16}=G_{xy}(000,-;210,+;\omega^2),$$
$$g_{17}=G_{yy}(000,-;210,+;\omega^2),$$
$$g_{18}=G_{zz}(000,-;210,+;\omega^2),$$
$$g_{19}=G_{xx}(000,+;220,+;\omega^2),$$
$$g_{20}=G_{xy}(000,+;220,+;\omega^2),$$
$$g_{21}=G_{xx}(000,+;211,+;\omega^2),$$
$$g_{22}=G_{xy}(000,+;211,+;\omega^2),$$
$$g_{23}=G_{yz}(000,+;211,+;\omega^2),$$
$$g_{24}=G_{xx}(000,+;310,+;\omega^2),$$
$$g_{25}=G_{xy}(000,+;310,+;\omega^2),$$
$$g_{26}=G_{yy}(000,+;310,+;\omega^2).$$

For the cation-pair impurity the $\underline{g}$ matrix can be written in terms of similar 26 Green's functions obtained from the above by an interchange of plus and minus signs. g_1, for example, is now $G_{\alpha\beta}(000,+;000,+;\omega^2)$ instead of being $G_{\alpha\beta}(000,-;000,-;\omega^2)$, and so on.

The perturbation matrix J contains the mass changes and the changes in the short-range forces at the defect sites. The short-range forces can be expressed in terms of Kellerman[17] coefficients A and B. To make the situation simple we assume that there is no relaxation around the defect ions making the changes in B to be zero.

Let ΔA be the A parameter for the defect-host bond minus the A parameter for the perfect lattice, and ϵM be the mass of the substituted host ion minus the mass of the substituting defect ion. The elements of the J matrix are then written in

terms of the following two quantities:

$$J_1 = \epsilon M\omega^2 + 2\Delta A, \quad J_2 = \Delta A .$$

ANALYTICAL FORMULAS

Analytical expressions obtained for computation of the three infrared-active modes and the three Raman-active modes after block-diagonalizing the 36×36 $(\underline{I} - \underline{g}\underline{J})$ matrix are given below.

B_{1U} mode (transverse infrared-active mode)—defect ions moving inphase in [001] *direction.* The mode frequencies are given by the determinantal equation

$$|B_{1U}| = 0 .$$

As noted earlier, $|B_{1U}|$ is a 5×5 determinant, but in view of several of its elements being zeros, it is seen to be equal to a 2×2 determinant whose elements are given below:

$$b_{11} = 1 - J_1(g_1 - g_7) + 2J_2(g_3 + g_{11}) ,$$

$$b_{12} = \sqrt{2}J_2(g_1 + g_7 - g_5 - g_{11}) ,$$

$$b_{21} = \sqrt{2}J_2(g_2 + g_{13} + g_{10} + g_{21}) - \sqrt{2}J_1(g_3 + g_{11}) ,$$

$$b_{22} = 1 + J_2(2g_3 - g_2 - g_{13} + 2g_{11} - g_{10} - g_{21}) .$$

B_{2U} mode (longitudinal infrared-active mode)—defect ions moving inphase in [110] *direction.* The mode frequencies are given by the determinantal equation

$$|B_{2U}| = 0 .$$

Here $|B_{2U}|$ is a 6×6 determinant, but it is found to be equal to a 4×4 determinant owing to several of its elements being zero. The elements of the 4×4 determinants are as follows:

$$C_{11} = 1 - J_1(g_1 + g_5 + g_6) + J_2(2g_3 + g_4 + g_{15} + g_{16}) ,$$

$$C_{12} = (J_2/\sqrt{2})(g_5 + g_6 + g_1 - g_3 - g_{15} - g_{16}) ,$$

$$C_{13} = J_2(g_1 + g_5 + g_6 - g_3 + g_4) ,$$

$$C_{14} = 2J_2 g_{12} ,$$

$$C_{21} = \sqrt{2}J_2(g_2 + g_8 + g_{20} + g_{13} + g_{24}) - \sqrt{2}J_1(g_3 + g_{15} + g_{16}) ,$$

$$C_{22} = 1 + J_2(g_3 - g_2 + g_9 - g_{24} + g_{15} + g_{16} - g_{20}) ,$$

$$C_{23} = J_2\sqrt{2}(g_3 - g_8 - g_9 + g_{15} + g_{16} - g_{13}) ,$$

$$C_{24} = 2\sqrt{2}J_2(g_{22} - g_9) ,$$

$$C_{31} = J_2(g_2 + 2g_8 + g_{13}) - J_1(g_3 + g_4) ,$$

$$C_{32} = (J_2/\sqrt{2})(g_3 + g_4 - g_8 - g_9 - g_{13}) ,$$

$$C_{33} = 1 - J_2(g_2 + g_8 - g_9 - g_3 - g_4) ,$$

$$C_{34} = 2J_2 g_9 ,$$

$$C_{41} = 2J_1 g_{12} - 2J_2 g_{22} ,$$

$$C_{42} = \sqrt{2}J_2(g_{22} - g_{12} - g_9) ,$$

$$C_{43} = 2J_2(g_9 - g_{12}) ,$$

$$C_{44} = 1 + J_2(g_{13} + g_{10} - g_2 - g_{21}) .$$

B_{3U} mode (transverse infrared-active mode)—defect ions moving inphase in [110] *direction.* The mode frequencies are given by the determinantal equation

$$|B_{3U}| = 0 .$$

Here $|B_{3U}|$ is a 5×5 determinant but in view of several of its elements being zero, it is seen to be equal to a 3×3 determinant whose elements are given below:

$$d_{11} = 1 - J_1(g_1 + g_5 - g_6) + J_2(2g_3 + g_{15} - g_{16} + g_4) ,$$

$$d_{12} = (J_2/\sqrt{2})(g_1 + g_5 - g_6 - g_3 - g_{15} + g_{16}) ,$$

$$d_{13} = J_2(g_1 + g_5 - g_6 - g_3 - g_4) ,$$

$$d_{21} = -\sqrt{2}J_1(g_3 + g_{15} - g_{16}) + J_2\sqrt{2}(g_2 + g_8 + g_{13} + g_{24} - g_{20}) ,$$

$$d_{22} = 1 - J_2(g_2 - g_3 + g_9 - g_{20} + g_{15} - g_{16} + g_{24}) ,$$

$$d_{23} = J_2\sqrt{2}(g_{15} - g_{16} + g_3 - g_8 + g_9 - g_{13}) ,$$

$$d_{31} = J_2(g_2 + g_{13} + 2g_8) - J_1(g_3 + g_4) ,$$

$$d_{32} = (J_2/\sqrt{2})(g_3 + g_4 - g_8 + g_9 - g_{13}) ,$$

$$d_{33} = 1 - J_2(g_2 - g_3 - g_4 + g_8 + g_9) .$$

A_g mode (Raman-active longitudinal mode)—defect ions moving out of phase in [110] *direction.* The mode frequencies are given by the determinantal equation

$$|A_g| = 0 .$$

Here $|A_g|$ is a 6×6 determinant, but in view of several of its elements being zero, it is seen to be equal to a 4×4 determinant whose elements are given below:

$$A_{11} = 1 + J_1(g_5 + g_6 - g_1) + J_2(2g_3 - g_{15} - g_{16} - g_4) ,$$

$$A_{12} = (J_2/\sqrt{2})(g_1 - g_5 - g_6 - g_3 + g_{15} + g_{16}) ,$$

$$A_{13} = J_2(g_3 - g_4 + g_5 + g_6 - g_1) ,$$

$$A_{14} = -2J_2 g_{12} ,$$

$$A_{21} = +\sqrt{2}J_1(g_{15} + g_{16} - g_3) - \sqrt{2}J_2(g_8 + g_{24} + g_{20} - g_2 - g_{13}) ,$$

$$A_{22} = 1 - J_2(g_2 - g_3 - g_9 + g_{15} + g_{16} - g_{20} - g_{24}) ,$$

$$A_{23} = J_2\sqrt{2}(g_{13} + g_{15} + g_{16} - g_8 + g_9 - g_3) ,$$

$$A_{24} = -2\sqrt{2}J_2(g_9 + g_{22}) ,$$

$$A_{31} = J_1(g_3 - g_4) - J_2(g_2 + g_{13} - 2g_8) ,$$

$$A_{32} = (J_2/\sqrt{2})(g_4 + g_{13} - g_8 + g_9 - g_3) ,$$

$$A_{33} = 1 - J_2(g_2 - g_3 - g_8 - g_9 + g_4) ,$$

$$A_{34} = -2J_2 g_9 ,$$

$$A_{41} = -2J_1 g_{12} + 2J_2 g_{22} ,$$

$$A_{42} = \sqrt{2}J_2(g_{12} - g_{22} - g_9) ,$$

$$A_{43} = -2\sqrt{2}(g_{12} + g_9) ,$$

$$A_{44} = 1 - J_2(g_2 - g_{13} - g_{21} + g_{10}) .$$

B_{1g} mode (transverse Raman-active mode)—defect ions vibrating out of phase in the [$\bar{1}$10] direction. The mode frequencies are given by the determinantal equation

$$|B_{1g}| = 0 .$$

Here $|B_{1g}|$ is a 5×5 determinant, but in view of several of its elements being zero, it is seen to be equal to a 3×3 determinant whose elements are given below:

$$B_{11} = 1 - J_1(g_1 - g_5 + g_6) - J_2(2g_3 + g_4 + g_{15} - g_{16}) ,$$
$$B_{12} = (J_2/\sqrt{2})(g_{15} - g_{16} - g_5 + g_6 - g_1 - g_3) ,$$
$$B_{13} = J_2(g_3 - g_4 + g_5 - g_6 - g_1) ,$$
$$B_{21} = J_2\sqrt{2}\,(g_2 + g_{13} - g_8 + g_{20} - g_{24}) - \sqrt{2}J_1(g_3 - g_{15} + g_{16}) ,$$
$$B_{22} = 1 - J_2(g_2 - g_3 + g_9 + g_{15} - g_{16} + g_{20} - g_{24}) ,$$
$$B_{23} = \sqrt{2}\,J_2(g_{13} - g_3 - g_8 - g_9 + g_{15} - g_{16}) ,$$
$$B_{31} = 2J_1(g_3 - g_4) + J_2(2g_8 - g_2 - g_{13}) ,$$
$$B_{32} = (J_2/\sqrt{2})(g_4 - g_3 - g_8 - g_9 + g_{13}) ,$$
$$B_{33} = 1 - J_2(g_4 + g_2 - g_3 - g_8 + g_9) .$$

B_{3g} mode (transverse Raman-active mode)—defect ions moving out of phase in [001] direction. The mode frequencies are given by the determinantal equation

$$|B_{3g}| = 0 .$$

Here $|B_{3g}|$ is a 4×4 determinant but in view of several of its elements being zero, it is seen to be equal to a 2×2 determinant whose elements are given below:

$$T_{11} = 1 - J_1(g_1 - g_7) + 2J_2(g_3 - g_{11}) ,$$
$$T_{12} = J_2(g_1 + g_{11} - g_3 - g_1) ,$$
$$T_{21} = J_1\sqrt{2}\,(g_{11} - g_3) + J_2\sqrt{2}\,(g_2 + g_{13} - g_{10} - g_{21}) ,$$
$$T_{22} = 1 - J_2(g_2 + g_{13} + 2g_{11} - 2g_3 - g_{10} - g_{21}) .$$

RESULTS AND DISCUSSION

Inspection of the normal coordinates reveals that the three modes B_{1U}, B_{2U}, and B_{3U} are ir-active while the remaining three B_{1g}, B_{2g}, and B_{3g} are Raman active. Further, B_{2U} and A_g are seen

TABLE I. Local-mode frequencies (in cm^{-1}) of H^-–H^- pair impurities in the [110] direction in KCl, KBr, KI, NaCl, RbCl, and of D^-–D^- pair impurities in the [110] direction in KCl and KBr.

System	ΔA (in units of $e^2/2$ V)	Infrared-active modes: B_{2U} (L mode) Calc.	Expt.	B_{3U} (T_1 mode) Calc.	Expt.	B_{1U} (T_2 mode) Calc.	Expt.	Raman-active modes: A_g (L mode) Calc.	Expt.	B_{1g} (T_1 mode) Calc.	Expt.	B_{3g} (T_2 mode) Calc.
	−4.88	464.53		538.14		521.17		543.8		484.7		490.76
KCl:H^-–H^-	−4.92	462.08	463.5	535.87	535	518.79	512.5	541.46	···	482.46	···	488.26
	−4.96	459.25		533.57		516.39		538.14		479.96		484.44
	−5.3	409.66		481.05		472.89		491.55		440.04		432.94
KBr:H^-–H^-	−5.4	402.78	402.4	475.39	496.5 488.4 482.0 476.2	466.06	457.2	485.52	···	434.61	···	426.77
	−5.5	396.0		471.38		462.07		481.08		429.06		418.52
	−6.87	328.93		392.1		388.15		405.33		371.76		351.63
KI:H^-–H^-	−6.89	327.69	324.0	391.07	424.8	387.05	390.3	404.31	···	370.55	···	350.50
	−6.91	326.39		390.0		385.87		403.28		369.67		349.3
	−4.59	492.48		603.03		604.5		651.94		571.27		552.2
NaCl:H^-–H^-	−4.63	488.97	497.4	600.22	600.0	601.62	583.2	649.35	···	568.64	···	549.14
	−4.67	485.32		597.14		598.8		646.8		565.95		546.06
	−5.66	446.71		515.06		505.38		524.67		465.36		470.48
RbCl:H^-–H^-	−5.68	445.44	445.5	514.00	515.6	504.27	482.9	523.63	···	464.22	···	469.32
	−5.70	444.19		512.92		502.16		522.61		463.1		468.17
	−4.93	328.76		382.0		369.86		386.0		352.16		347.72
KCl:D^-–D^-	−4.97	326.65	331.5	380.21	375.5	368.25	368.0	384.6	···	350.8	···	345.92
	−5.01	324.47		378.6		366.64		383.0		349.3		343.96
	−5.3	291.07		341.96		336.29		351.31		324.45		309.09
KBr:D^-–D^-	−5.4	286.19	287.1	338.05	342.9	332.24	328.4	347.49	···	321.16	···	304.65
	−5.5	281.33		333.94		328.32		343.62		317.88		300.18

to be longitudinal modes, whereas the remaining four are transverse modes. Using the analytical expressions of the preceding section, the computation was carried out on the TDC-12 computer at the Faculty of Engineering, University of Jodhpur, Jodhpur. Required Green's functions computed on the bases of neutron-fitted shell-model parameters[18-20] were used. A variable force constant approach has been followed. Table I shows the computed ir-active as well as the Raman-active modes for the systems $KCl:H^--H^-$, $KBr:H^--H^-$, $KI:H^--H^-$, $NaCl:H^--H^-$, $RbCl:H^--H^-$, $KCl:D^-D^-$, and $KBr:D^-D^-$. The experimental values of the ir-active local-mode frequencies reported by de Souza *et al.*[5-7] are also displayed in the same table. Raman-active modes in these systems have not been reported so far, but our theoretical prediction will be useful for future experiments, whenever carried out in these systems. One can notice a very good agreement between the observed and the calculated ir-active local modes for the system $KCl:H^-H^-$ at $\Delta A = -4.92$ (in units of $e^2/2V$ of KCl). Likewise for the systems $KBr:H^-H^-$, $KI:H^-H^-$, $NaCl:H^-H^-$, $RbCl:H^-H^-$, $KCl:D^-D^-$, and $KBr:D^-D^-$, good agreement between the observed and calculated ir-active local mode at ΔA (in units of $e^2/2V$ of respective host crystals) $= -5.4$, -6.89, -4.63, -5.68, -4.97, and -5.4, respectively. At these values of ΔA, the computed resonant modes are displayed in Table II. It may be recalled that for localized modes the mode frequencies are greater than ω_L, while for resonant modes, the mode frequencies are less than ω_L. Here ω_L denotes the maximum frequency for the phonon propagation in the perfect crystal. For example, in the case of KCl, ω_L is 216 cm^{-1}. The roots of the determinantal equation $|\underline{I} - \underline{G}\underline{J}| = 0$ which are greater than ω_L are the local-mode frequencies, while the remaining are the resonant-mode frequencies.

Table III shows the computed gap modes together with the experimentally observed[10] ir-active modes due to Cl^-, Br^-, and Na^+ ion pairs in KI. In the case of KI, the frequency band from 71 to 94 cm^{-1}

TABLE II. Calculated resonant-mode frequencies (in cm^{-1}) for the systems $KCl:H^-H^-$, $KCl:D^-D^-$, $KBr:H^-H^-$, $KBr:D^-D^-$, $NaCl:H^-H^-$, $KI:H^-H^-$, and $RbCl:H^-H^-$.

	Infrared-active modes			Raman-active modes		
System	B_{2U} (L mode)	B_{3U} (T_1 mode)	B_{1U} (T_2 mode)	A_g (L mode)	B_{1g} (T_1 mode)	B_{3g} (T_2 mode)
$KCl:H^-H^-$	145.12	146.78	145.89	149.42	63.6	148.29
					143.96	
					144.96	
					148.62	
$KCl:D^-D^-$	145.11	148.01	145.97	149.61	64.14	148.30
					141.86	
					146.06	
					152.87	
$RbCl:H^-H^-$	125.12	146.82	142.83	143.7	50.04	128.12
					127.42	
$NaCl:H^-H^-$	127.74	139.52	171.4	99.68	92.87	175.79
	139.34	177.67		105.00	132.49	
	170.83			131.19	139.34	
				139.34	159.83	
				177.27		
$KBr:H^-H^-$	69.81	84.21	82.93	83.08	44.41	72.8
	106.6	98.0	99.89	98.5	84.48	82.0
	119.56	106.22	119.3	106.21	95.00	98.84
	126.63	119.19		123.3	103.0	
	135.0			135.81		
$KBr:D^-D^-$	69.94	98.00	82.96	83.08	44.54	72.8
	106.61	106.22	99.91	98.5	84.68	82.08
	119.56	119.19	119.28	106.2	95.1	98.84
	126.6	135.14		123.31		
	134.64			135.55	103.0	
$KI:H^-H^-$	8.33	61.78	55.4	55.92	37.78	52.5
	51.9	83.7	61.35	83.75	62.7	84.27
	61.4	96.05	84.3	84.17	69.75	102.0
	92.83		94.0	90.36	83.7	
				96.0		

TABLE III. Gap modes (in cm^{-1}) due to Cl^-, Br^-, and Na^+ ion pairs in the [110] direction in KI.

System	ΔA (in units of $e^2/2$ V)	Infrared-active modes: B_{2U} (L mode) Calc.	Expt.	B_{3U} (T_1 mode) Calc.	Expt.	B_{1U} (T_2 mode) Calc.	Expt.	Raman-active modes: A_g (L mode) Calc.	Expt.	B_{1g} (T_1 mode) Calc.	Expt.	B_{3g} (T_2 mode) Calc.
	1.5	76.0		79.81		80.99		83.27		86.96		79.03
KI:Cl^-–Cl^-	0.5	75.81	72.02	79.73	80.26	80.96	82.84	83.16	...	82.25	...	78.98
	−0.5	75.6		79.61		80.65		83.04		78.15		78.75
	−12.0	72.47		72.46		78.88		73.0		72.4		77.28
		75.48		77.44				79.41				
		89.57						89.58				
KI:Br^-–Br^-	−13.0	71.5	73.65	71.44	...	78.29	...	71.7	...	70.26	...	76.74
		75.4	86.97	76.79				79.0				
		86.84						87.44				
	−14.0	73.94				77.79		70.26		...		76.19
		84.47		76.47				78.55				
								85.32				
	−5.55	79.26		84.84		84.49		87.21		92.62		82.42
KI:Na^+–Na^+	−5.65	78.09	76.02	83.92	84.1	83.65	...	86.46	...	92.39	...	81.33
	−5.75	76.76		82.81		82.64		85.59		91.7		80.23

is a forbidden band for phonon propagation, although the maximum frequency of phonon propagation is 142 cm^{-1}. This gap between the acoustical and optical band is ascertained from the fact that throughout this frequency band the imaginary part of the Green's function is zero. It is seen from Table III that the computed ir-active modes are in good agreement with the observed ir-active modes, when $A = 0.5$, -13.0, -5.65, respectively, for the systems KI : Cl^-–Cl^-, KI : Br^-–Br^-, and KI : Na^+–Na^+. At these values of ΔA parameters, the computed resonant modes are displayed in Table IV.

Table V shows the computed and experimentally observed resonant modes for the system KCl : Na^+–Na^+, NaCl : F^-–F^-, and NaCl : Ag^+–Ag^+. For the system KCl : Na^+–Na^+ only one ir-active resonant mode frequency 44 cm^{-1} has been reported[9] so far, which is in excellent agreement with one of the computed B_{3U} modes (43.95 cm^{-1}) at $\Delta A = -6.0$. In the case of NaCl : F^-–F^- Becker and Martin[8] observed six ir-active local modes, namely, 32.7, 38.0, 40.2, 44.7, 48.4, and 72.0 cm^{-1}. They suggested the existence of these modes was due to the presence of F^-–F^- ion pairs in two configurations, namely [110] and [200]. Our calculation of the B_{2U} mode at $\Delta A = -5.94$ agrees very well with four out of these six modes; the remain-

TABLE IV. Calculated resonant-mode frequencies (in cm^{-1}) for the systems KI:Cl^-–Cl^-, KI:Br^-–Br^-, and KI:Na^+–Na^+.

System	Infrared-active modes: B_{2U} (L mode)	B_{3U} (T_1 mode)	B_{1U} (T_2 mode)	Raman-active modes: A_g (L mode)	B_{1g} (T_1 mode)	B_{3g} (T_2 mode)
KI:Cl^-–Cl^-	52.7	62.53	55.79	62.2	52.5	57.28
			62.03			98.89
			110.36			108.02
			117.54			
KI:Br^-–Br^-	13.65	18.18	55.4	44.51	38.66	54.44
	41.87	43.27	61.73	55.5	54.0	95.24
	51.76	62.26	98.41	61.33	62.71	117.63
					69.42	
KI:Na^+–Na^+	48.55	...	49.95	35.34	40.23	39.77
				50.92		50.5
				97.74		
				98.24		

TABLE V. Resonant-mode frequencies (in cm^{-1}) for the systems $NaCl:F^-{-}F^-$, $NaCl:Ag^+{-}Ag^+$, and $KCl:Na^+{-}Na^+$.

System	ΔA (in units of $e^2/2$ V)	Infrared-active modes						Raman-active modes					
		B_{2U} (L mode)		B_{3U} (T_1 mode)		B_{1U} (T_2 mode)		A_g (L mode)		B_{1g} (T_1 mode)		B_{3g} (T_2 mode)	
		Calc.	Expt.	Calc.	Expt.	Calc.	Expt.	Calc.	Expt.	Calc.	Expt.	Calc.	Expt.
	−5.96	23.75		91.34		52.4		58.47		79.07		67.74	
		30.5		146.14		60.37		147.76		124.74		105.12	
		85.07				80.4				147.48		147.7	
		103.09				104.33				153.52			
		112.9				145.55				164.78			
		145.44											
$KCl:Na^+{-}Na^+$	−6.0	58.08	···	37.39	44.0	84.08	···	45.7	···	81.81	···	102.98	···
		93.59		43.95		102.95		105.55		88.00		110.12	
		113.94		95.91		111.06		148.7		114.5		148.12	
		146.18		146.77		146.16				119.31		157.4	
										149.5			
										167.74			
	−6.04	31.62		90.5		61.28		57.35		78.53		51.94	
		83.96		146.12		80.5		147.37		147.57		66.84	
		103.93				86.15				153.51		106.0	
		113.3				105.78				165.1		147.77	
		145.46				145.56							
	−4.94	23.7		106.0		65.12		73.75		115.3		87.62	
		49.0		130.05		122.54		130.25		141.04		174.21	
		83.25		140.14		129.95		140.94		175.28			
		89.02		171.29		170.67		176.27		182.72			
		94.15								199.5			
		120.45											
$NaCl:F^-{-}F^-$	−5.0	24.4	32.7	105.0	···	63.69	···	72.58		116.74	···	87.07	···
		33.1	38.0	130.05		123.16		130.19		141.0		174.32	
		38.6	44.7	140.19		129.77		140.97		175.36			
		47.67	48.4	171.3		170.71		176.36		182.64			
		50.92								199.0			
		80.87											
	−5.06	14.34		104.21		62.22		71.49		117.55		88.53	
		20.98		129.94		123.98		130.09		140.88		174.5	
		41.21		140.24		129.6		141.0		175.46			
		51.34		171.4		170.74		176.45		182.6			
		79.54								199.5			
		121.12											
	−2.9	42.74		49.09		48.34		52.04		167.7		48.34	
		167.38		50.96		169.16		179.79				174.5	
				56.79									
				172.17									
$NaCl:Ag^+{-}Ag^+$	−3.1	39.95	···	48.27	···	47.29	···	51.59	···	168.27	···	47.22	47.0
		167.59		52.1		169.31		179.81				174.56	
				56.4									
				172.27									
	−3.3	37.49		47.44		46.21		51.08		168.95		46.0	
		167.77		53.0		169.45		179.81				174.77	
				56.0									
				172.27									

ing two should be explained by another theoretical calculation taking $F^-{-}F^-$ pairs in the [200] configuration. In the case of the system $NaCl:Ag^+{-}Ag^+$, our calculated Raman-active B_{3g} mode (47.22) at $\Delta A = -3.1$ is in excellent agreement with the observed mode[11] (47.0).

Table VI shows the ir-active as well as the Raman-active gap modes for the system $KI:Rb^+{-}Rb^+$ calculated by using a Green's-function technique together with the values calculated by Ward and Clayman[12] using the molecular-model method. A general agreement between the results

TABLE VI. Calculated gap modes (in cm^{-1}) due to Rb^+ ion pairs in the [110] direction in KI. The values of the ΔA parameters indicated are in units of $e^2/2$ V of KI.

Mode	Calculation $\Delta A = 0$	$\Delta A = 2.0$	$\Delta A = 4.0$	Calculation of Ward and Clayman [a]
A_g	70.94	87.42	92.33	85.99
B_{1g}	76.69	81.73	86.95	84.64
B_{3g}	78.0	85.4	91.35	90.7
B_{1U}	78.67	86.0	91.95	88.19
B_{2U}	77.06	84.43	90.98	83.05
B_{3U}	80.16	87.62	92.46	89.0

[a] Reference 12.

of two calculations can be noticed. No experimental results are, however, available in this system.

CONCLUSION

We conclude that the Green's-function technique is most suitable for the theoretical calculations, due to a point defect in an otherwise perfect crystal. The molecular-model method, treating the impurity and its nearest neighbor as a vibrating molecule, gives only the local-mode frequencies, whereas the Green's-function technique provides both localized and resonant modes. We note from the present calculation that the effect of introducing defect ion pairs is mostly to reduce the coupling constant considerably, although in some cases no change in coupling constant or little enhancement is noticed. The change in the force constant due to the H^-–H^- ion pairs and D^-–D^- ion pair is the same in case of KBr ($\Delta A = -5.4$ in both cases). In case of KCl also, the H^-–H^- ion pair and D^-–D^- ion pair produce nearly the same reduction of the force constant ($\Delta A = -4.92$ for H^-–H^- ion pair and $\Delta A = -4.97$ for D^-–D^- ion pair). This is to be expected because D^- ion is roughly two times heavier than the H^- ions and the observed frequency due to single H^- ion in KCl and KBr (502 and 446 cm^{-1}, respectively) are roughly $\sqrt{2}$ times the observed frequencies due to a single D^- ion in KCl and KBr (360 and 318 cm^{-1}, respectively). The importance of these calculations thus lies in formulating a consistent theory for the interatomic force constants in ionic crystals. It is hoped these Raman-active modes and the resonant modes predicted in this paper will be useful for future experiments on these systems.

*Currently on deputation at the Dept. of Basic Sciences and Humanities, Arab Gulf Academy, Basarah, Iraq.

[1] A. J. Sievers, *Localized Excitations in Solids*, R. F. Wallis (Plenum, New York, 1968), p. 27.
[2] R. F. Wallis, in Ref. 1.
[3] A. A. Maradudin, *Elementary Excitations in Solids*, edited by A. A. Maradudin and G. F. Nardelli (Plenum, New York, 1968).
[4] M. V. Klein, in *Physics of Color Centers*, edited by W. B. Fowler (Academic, New York, 1968) Chap. 7, p. 436.
[5] M. de Souza, A. D. Gongora, M. Aegerter, and F. Lüty, Phys. Rev. Lett. 25, 1426 (1970).
[6] M. de Souza and F. Lüty, Phys. Rev. B 8, 5866 (1973).
[7] R. Robert and M. de Souza, Phys. Rev. B 9, 5257 (1974).
[8] C. R. Becker and T. P. Martin, Phys. Rev. B 5, 1604 (1972).
[9] T. L. Templeton and B. P. Clayman, Solid State Commun. 9, 697 (1971).
[10] R. W. Ward and B. P. Clayman, Phys. Rev. B 9, 4455 (1974).
[11] W. Moller, R. Kaiser, and H. Bilz, Phys. Lett. A32, 171 (1970).
[12] R. W. Ward and B. P. Clayman, Can. J. Phys. 52, 1492 (1974).
[13] T. M. Haridasan, R. K. Gupta, and W. Ludwig, Chem. Phys. Lett. 23, 217 (1973).
[14] T. M. Haridasan, R. K. Gupta, and W. Ludwig, Solid State Commun. 12, 1205 (1973).
[15] R. K. Gupta, P. Mathur, and A. K. Singh, J. Phys. Chem. Solids 38, 809 (1977).
[16] A. A. Maradudin, E. W. Montroll, G. H. Weiss, and I. P. Ipatova, *Theory of Lattice Dynamics in Harmonic Approximation* (Academic, New York, 1971).
[17] E. W. Kellerman, Philos. Trans. R. Soc. London Ser. A 238, 513 (1940).
[18] G. Raunio and S. Rolandson, Phys. Rev. B 2, 2098 (1976).
[19] R. A. Cowley, W. Cochran, B. N. Brockhouse, and A. D. B. Woods, Phys. Rev. 131, 1038 (1963).
[20] G. Dolling, R. A. Cowley, C. Schittenheln, and I. M. Thorson, Phys. Rev. 147, 577 (1966).